

Short Communication

Mechanical and Biological Properties of Biphasic Calcium Phosphate Scaffold depending on Different Nanoparticle Fabrication Methods

M.-H. Hong¹, S.-M. Kim², Y.-K. Lee^{*3}

¹Department of Neurosurgery, Spine and Spinal Cord Institute, Yonsei University College of Medicine, Seoul 03722, South Korea

²Department and Research Institute of Dental Biomaterials and Bioengineering, Yonsei University College of Dentistry, Seoul 03722, South Korea

³Research Center for Oral Disease Regulation of the Aged, Chosun University College of Dentistry and Graduate School of Dentistry, Gwangju 61452, South Korea

received May 19, 2017; received in revised form August 30, 2017; accepted November 6, 2017

Abstract

Biphasic calcium phosphate (BCP) is widely used as biomaterial for bone regeneration because of its favourable bioactivity and bioresorption property when compared to hydroxyapatite and β -tricalcium phosphate on their own. Two types of BCP are available in orthopedics and dentistry: chemically synthesized BCP (C-BCP) and mechanically mixed BCP (M-BCP). In this study, the mechanical and biological properties of these two types of BCP scaffold were compared. The scaffolds were characterized based on an evaluation of their surface morphology by means of SEM, and their compressive strength was determined in a universal testing machine. The cell proliferation and osteogenic differentiation were measured in a cell-counting assay and alkaline phosphatase activity test. Compared to the M-BCP scaffold, the C-BCP scaffold showed enhanced compressive strength owing to the dense surface of struts. However, the C-BCP and M-BCP scaffolds were shown to be similar with regard to biological properties. This study concluded that the method applied to fabricate BCP nanoparticles influenced their size, the smaller size particles resulting in good mechanical properties thanks to their dense surface. However, the particle size did not influence the biological properties of the BCP scaffolds.

Keywords: Calcium phosphates, scaffolds, mechanical property, biological property

I. Introduction

Calcium phosphates (CaPs) are known as excellent biomaterials in biomedical science and engineering thanks to their high biocompatibility, bioactivity and osteoconductivity. Of the CaPs, hydroxyapatite (HAp; $\text{Ca}_{10}(\text{PO}_4)_6(\text{OH})_2$) and β -tricalcium phosphate (β -TCP; $\text{Ca}_3(\text{PO}_4)_2$) are most widely used in dental and orthopedic fields. HAp is known as a good reconstructive material in bone substitute applications owing to properties like similar calcium and phosphate ratio (Ca/P) to that of natural bone and higher biocompatibility and bioactivity. However, many studies have indicated that the degradation rate of HAp in the human body is too low to achieve optimal results¹. β -TCP has been shown to have a higher degradation rate than HAp. This rapid degradation profile drastically reduces the surface area available for cell proliferation and its application in the clinical setting is therefore limited². Biphasic calcium phosphate (BCP) consists of HAp and β -TCP and has been researched with the aim of combining the advantages of CaPs. BCP has been recommended for use as drug delivery, bone substitute and dental applica-

tions because of its biocompatibility and biodegradability. There is growing interest in developing BCP as a scaffolding material because it is more effective in hard tissue regeneration than pure HAp or pure β -TCP, and has, to a certain degree, a controllable degradation rate³.

CaPs have been synthesized with various methods such as solid-state reaction^{4,5}, precipitation^{6,7}, and sol-gel methods^{8,9}. The sol-gel method is regarded as a promising route for synthesis because of the limited equipment required, high output and easy operation⁸. Specifically, the sol-gel method has been researched in various applications for the fabrication of nanoparticles. Some previous studies have reported that a smaller particle size can significantly enhance the mechanical and biological properties^{10,11}. Crystalline CaP nanoparticles exhibit improved sinterability and enhanced densification owing to their larger surface area, which may improve fracture toughness, as well as other mechanical properties¹⁰. The smaller, less crystalline CaPs nanoparticles increase cellular adhesion and growth compared to larger and more crystalline CaP nanoparticles¹¹. CaPs have been shown to exhibit a low mechanical property of being brittle, however, the me-

* Corresponding author: leeyk0129@chosun.ac.kr

chanical and biological properties of the nanoparticles have been enhanced.

The aim of this study is to fabricate and evaluate two types of BCP scaffold using different sized nanoparticles prepared with different methods; mechanically mixing of HAp and β -TCP in a ball mill and synthesis of chemically calcium nitrate tetrahydrate and triethoxy phosphate with the sol-gel method. Each scaffold was fabricated by means of template-casting methods using BCP nanoparticles prepared with different methods and compared in terms of the mechanical and biological properties of the BCP scaffolds.

II. Materials and Methods

HAp, β -TCP and chemically synthesized BCP (C-BCP) nanoparticles were prepared with a sol-gel method in which the calcium nitrate tetrahydrate (Sigma Aldrich, USA) and triethoxy phosphate (Sigma Aldrich, USA) used as starting materials were dissolved in methyl alcohol, followed by addition of deionized water and hydrochloric acid for hydrolysis. The Ca/P of each nanoparticle was controlled at about 1.67, 1.55 and 1.60. Calcium nitrate solution was heated up for partial dehydration in vacuum for 30 min and phosphate solution was hydrolyzed for two hours in argon atmosphere. A gel was formed from the prepared calcium nitrate tetrahydrate and triethoxy phosphate with adjustment to pH 10, and the reaction proceeded at 90 °C for a day. The residual materials were heated at 800 °C for phase transition¹². The mechanically mixed BCP (M-BCP) was prepared by mixing HAp with β -TCP in a ball mill for 24 h. The ratios of HAp and β -TCP in C-BCP and M-BCP were all controlled at 70:30, respectively. After preparation of C-BCP and M-BCP nanoparticles, they were characterized by means of X-ray diffraction (XRD) using an X-ray diffractometer with Cu K α radiation (Ultima IX, Rigaku, Japan). The functional groups of BCP nanoparticles were measured with Fourier-transform infrared (FT-IR; Avatar 360, Thermo, USA) spectroscopy. The size of the BCP nanoparticles was measured by means of laser diffraction (Nano-ZS90, Malvern, UK) where they were placed in distilled water and dispersed in an ultrasonic water bath.

For the fabrication of C-BCP and M-BCP scaffolds ($5 \times 5 \times 5$ mm³), two types of slurry were prepared by dispersing the prepared C-BCP and M-BCP nanoparticles into distilled water with organic additive (5 % polyvinyl alcohol, 1 % methyl cellulose, 5 % ammonium polyacrylate dispersant, and 5 % N, N-dimethylformamide drying agent)¹³. The polyurethane (PU) sponge, 45-ppi (pores per inch) and with a pore diameter and porosity after sintering at 600–700 μ m and 75–80 % respectively, was used to fabricate a scaffold with fluid/gas-communicating channels that are observed in cancellous bone. The PU sponges were coated with prepared slurry and dried overnight. They were heated at 800 °C (heating rate 3 °K/min with dwelling time 1 h) and sintered at 1250 °C (heating rate 5 °K/min with dwelling time 3 h). The sintered scaffolds were coated again with slurry and resintered at 1250 °C (heating rate 5 °K/min with dwelling time 1 h)¹⁴. The sponge was selected and the sintering process was modified with reference to our previous study. The fabri-

cated scaffolds were characterized by evaluating their surface morphologies using a scanning electron microscopy (SEM; S-800, Hitachi, Japan) at an accelerating voltage of 20 kV. The compressive strength of the scaffolds was determined with a universal testing machine (3366, Instron®, USA) at 1 mm/min of the crosshead speed ($n = 3$). Briefly, a scaffold was loaded to fracture between two parallel compression plates. The plates were covered with a 0.5-mm-thick Parafilm® (Bemis, Neenah, USA) to eliminate any unexpected effects owing to an uneven horizontal surface level.

The cell proliferation and osteogenic differentiation were measured to determine the biological properties of C-BCP and M-BCP scaffolds. The MC3T3-E1 cells (pre-osteoblast cell line, ATCC, USA) were seeded on each scaffold (1×10^6 cells/mL) and incubated at 37 °C in a 5 % CO₂ incubator. The cell proliferation was measured by reducing dehydrogenases in cells using a WST-8 assay cell-counting Kit-8 (CKK-8; Dojindo Laboratories, Japan). The absorbance was read at 450 nm with an ELISA reader (Benchmark Plus, USA). The osteogenic differentiation was measured based on alkaline phosphatase (ALP) activity using Sensolyte® pNPP ALP assay Kit (Anaspec, USA). The absorbance was read at 405 nm with an ELISA reader. For the results, all the groups were reported as mean value \pm SD and statistically analyzed by *t*-test. The difference of each value was considered to be significant if *p*-values obtained in the test were less than 0.05.

III. Results and Discussion

Fig. 1a shows the XRD patterns of C-BCP and M-BCP nanoparticles. The main peaks of HAp (JCPDS No. 09–0432) and β -TCP (JCPDS No. 09–0169) were shown at around 31 and 32° (2 θ degree). From the results of XRD, the HAp to β -TCP ratio was determined as 60:40. For C-BCP and M-BCP nanoparticles, the FT-IR spectra showed OH⁻ absorption band at 3575 and 637 cm⁻¹ with the ν_3 and ν_4 bands of phosphate groups at 1049–1094 and 570–600 cm⁻¹, respectively (Fig. 1b). The above results show that the C-BCP and M-BCP nanoparticles were similar in terms of their chemical composition. However, from the size analysis results (Fig. 1c), the average of C-BCP and M-BCP nanoparticles was shown to be 477 nm and 255 nm, respectively. After the ball milling, the size was increased about twofold owing to the surface energy of nanoparticles. The nanoparticles with high surface energy tend to reduce their surface energy by agglomerating surrounding particles. Hence the increasing size trend during ball milling suggests a mechanism in the system that attempts to reverse the ever-increasing micro strain and specific surface energy of the grains¹⁵.

The struts and their surfaces of C-BCP and M-BCP scaffolds were shown with SEM (Fig. 2a). The struts of C-BCP and M-BCP scaffolds were shown in SEM images (Fig. 2a). The strut of C-BCP scaffold was denser than that of the M-BCP scaffold because of the smaller particle size. The results showed that the sinterability of the smaller-size BCP nanoparticles was much higher than that of the larger-size nanoparticles¹⁶, and this result influenced the mechanical property of the scaffold as mentioned below.

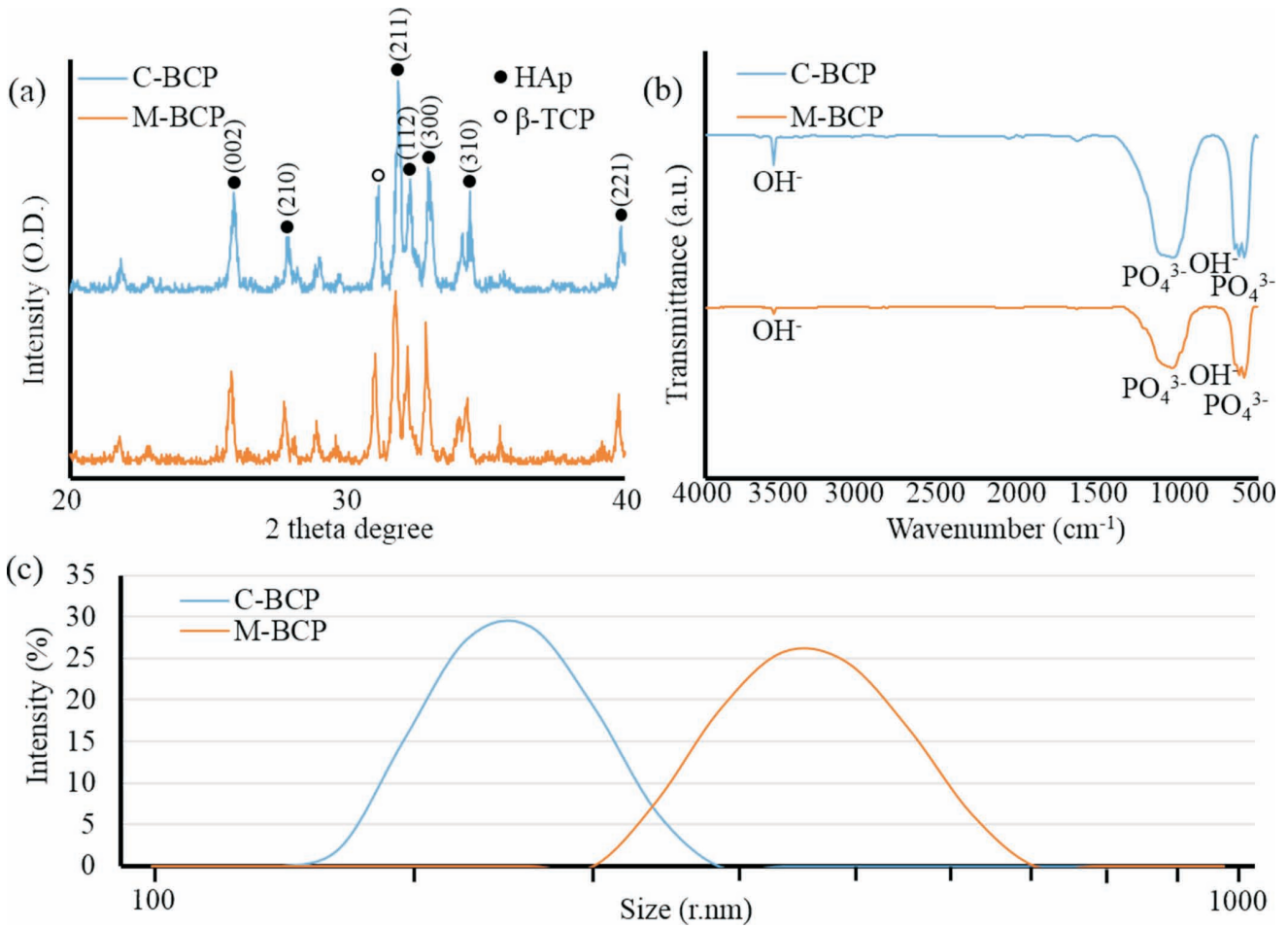


Fig. 1: (a) XRD patterns, (b) FT-IR patterns, and (c) particle sizes of C-BCP and M-BCP nanoparticles.

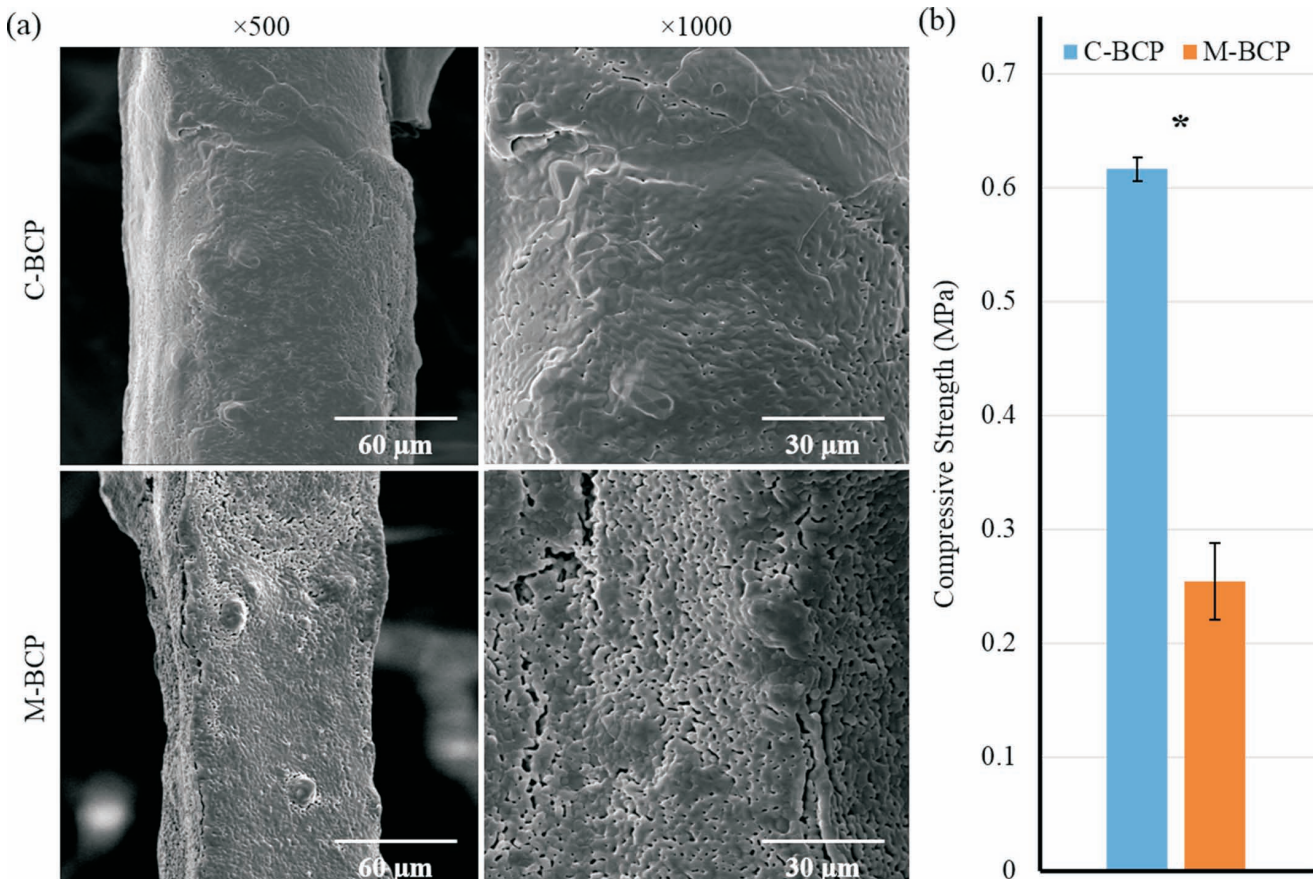


Fig. 2: (a) SEM images and (b) compressive strength of C-BCP and M-BCP scaffolds (*; expression of significant difference).

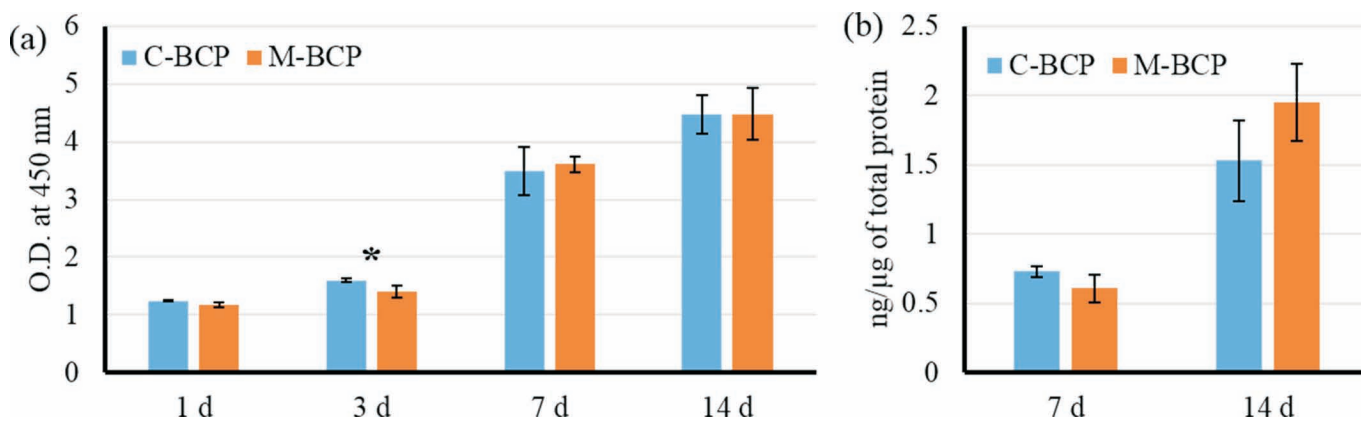


Fig. 3: (a) Cell proliferation and (b) osteogenic differentiation of C-BCP and M-BCP scaffolds (*; expression of significant difference).

The compressive strength was measured using a universal testing machine (Fig. 2b). The average compressive strength was 0.62 ± 0.03 and 0.25 ± 0.01 MPa for C-BCP and M-BCP scaffolds, respectively. The compressive strength of the C-BCP scaffold was about two times higher than that of the M-BCP scaffold and there was a significant difference ($p < 0.001$). In most other studies using smaller-size nanoparticles, compressive strength was increased about 1.5–2 times¹⁶. The mechanical strength was related to surface morphologies. The strut surface of C-BCP scaffold having dense, thicker and fewer pores was shown to have higher mechanical strength than the M-BCP scaffold.

Fig. 3a shows cell proliferation results during two weeks of culturing measured with CCK-8 assay. The optical density (O.D.) values were similar for C-BCP and M-BCP at all days. There was a significant difference only after three days ($p = 0.034$). This result means that the BCP scaffold fabricated with different particle sizes had no effect on cell proliferation rate for up to two weeks. Fig. 3b shows the osteogenic differentiation result based on measurement of the total protein and ALP activity at day 7 and 14. The results for C-BCP and M-BCP showed similar values for each day. Many previous researchers reported that the biological properties of the scaffold were affected by its porosity and pore size^{17,18}. However, from this study it was also identified that, while influencing the compressive strength, the particle size of BCP scaffolds had no effect on cellular proliferation and differentiation. Hence in the light of these results, it was concluded that although the BCP prepared with different fabrication methods leading to a different particle size resulted in a difference in compressive strength, no effect on biological properties was determined owing to the unchanged porosity and pore sizes.

V. Conclusions

Two types of BCP were successfully fabricated with different methods. The C-BCP was prepared with the sol-gel method, and the M-BCP was prepared by mixing HAP and β -TCP in a ball mill. Phase analysis of C-BCP and M-BCP showed them to be in a similar state. After each of the scaffolds had been fabricated, the C-BCP scaffold exhibited about twice the compressive strength than that of M-BCP owing to its particle size as this influenced its sinterability. However, the cell proliferation and osteogenic

differentiation results were similar over all days of monitoring. This study has shown that the method used to fabricate BCP has an effect on the mechanical property of a BCP scaffold whereas its biological properties are determined by other factors.

Acknowledgements

This work was supported by a National Research Foundation of Korea (NRF) grant funded by the Korean government (MSIP) (2016R1A6A3A11932752).

References

- 1 Kwon, S.H., Jun, Y.K., Hong, S.H., Kim, H.E.: Synthesis and dissolution behavior of beta-TCP and HA/beta-TCP composite powders, *J. Eur. Ceram. Soc.*, **23**, 1039–1045 (2003).
- 2 Kim, T.W. et al.: *In situ* formation of biphasic calcium phosphates and their biological performance in vivo, *Ceram. Int.*, **38**, 1965–1974, (2012).
- 3 Ramay, H.R.R., Zhang, M.: Biphasic calcium phosphate nanocomposite porous scaffolds for load-bearing bone tissue engineering, *Biomaterials*, **25**, 5171–5180, (2004).
- 4 Ryu, H.S. et al.: An improvement in sintering property of beta-tricalcium phosphate by addition of calcium pyrophosphate, *Biomaterials*, **23**, 909–914, (2002).
- 5 Guler, H., Gundogmaz, G., Kurtulus, F., Celik, G., Gacanoglu, S.S.: Solid state synthesis of calcium borohydroxyapatite, *Solid State Sci.*, **13**, 1916–1920, (2011).
- 6 Leng, Y., Chen, J.Y., Qu, S.X.: TEM study of calcium phosphate precipitation on HA/TCP ceramics, *Biomaterials*, **24**, 2125–2131, (2003).
- 7 Aimoli, C.G., Beppu, M.M.: Precipitation of calcium phosphate and calcium carbonate induced over chitosan membranes: A quick method to evaluate the influence of polymeric matrices in heterogeneous calcification, *Colloid Surface B*, **53**, 15–22, (2006).
- 8 Chen, J.D. et al.: A simple sol-gel technique for synthesis of nanostructured hydroxyapatite, tricalcium phosphate and biphasic powders, *Mater. Lett.*, **65**, 1923–1926, (2011).
- 9 Fellah, B.H., Layrolle, P.: Sol-gel synthesis and characterization of macroporous calcium phosphate bioceramics containing microporosity, *Acta Biomater.*, **5**, 735–742, (2009).
- 10 Zhou, H., Lee, J.: Nanoscale hydroxyapatite particles for bone tissue engineering, *Acta Biomater.*, **7**, 2769–2781, (2011).
- 11 Pathi, S.P., Lin, D.D.W., Dorvee, J.R., Estroff, L.A., Fischbach, C.: Hydroxyapatite nanoparticle-containing scaffolds for the study of breast cancer bone metastasis, *Biomaterials*, **32**, 5112–5122, (2011).

- 12 Zhang, S., Gonsalves, K.E.: Preparation and characterization of thermally stable nanohydroxyapatite, *J. Mater. Sci.-Mater. M*, **8**, 25–28, (1997).
- 13 Kim, S.M., Yi, S.A., Choi, S.H., Kim, K.M., Lee, Y.K.: Gelatin-layered and multi-sized porous beta-tricalcium phosphate for tissue engineering scaffold, *Nanoscale Res. Lett.*, **7**, 1–5, (2012).
- 14 Hong, M.H., Kim, S.M., Om, J.Y., Kwon, N., Lee, Y.K.: Seeding cells on calcium phosphate scaffolds using hydrogel enhanced osteoblast proliferation and differentiation, *Ann. Biomed. Eng.*, **42**, 1424–1435, (2014).
- 15 Nath, A.K., Jiten, C., Singh, K.C.: Influence of ball milling parameters on the particle size of barium titanate nanocrystalline powders, *Physica B*, **405**, 430–434, (2010).
- 16 Lin, K.L., Chen, L., Qu, H.Y., Lu, J.X., Chang, J.: Improvement of mechanical properties of macroporous beta-tricalcium phosphate bioceramic scaffolds with uniform and interconnected pore structures, *Ceram. Int.*, **37**, 2397–2403, (2011).
- 17 Kasten, P. *et al.*: Porosity and pore size of beta-tricalcium phosphate scaffold can influence protein production and osteogenic differentiation of human mesenchymal stem cells: An *in vitro* and *in vivo* study, *Acta Biomater.*, **4**, 1904–1915, (2008).
- 18 Byrne, D.P., Lacroix, D., Planell, J.A., Kelly, D.J., Prendergast, P.J.: Simulation of tissue differentiation in a scaffold as a function of porosity, Young's modulus and dissolution rate: Application of mechanobiological models in tissue engineering. *Biomaterials*, **28**, 5544–5554, (2007).

